J Biomol NMR (2007) 38:133–137
DOI 10.1007/s10858-007-9154-x

ARTICLE

Protein–protein interaction site mapping using NMR-detected mutational scanning

Bettina Baminger · Martin L. Ludwiczek · Georg Kontaxis · Stefan Knapp · Robert Konrat

Received: 9 October 2006 / Accepted: 12 March 2007 / Published online: 20 April 2007

Abstract We demonstrate a novel NMR method for the mapping of protein–protein interaction sites. In our approach protein–protein binding sites are mapped by competition binding experiments using indirect NMR reporter technology and Ala positional scanning. The methodology provides high sensitivity, ease of implementation and high-throughput capabilities. The feasibility of the technique is demonstrated with an application to the β-Catenin/Tcf4 complex.

Keywords Mutagenesis · NMR Spectroscopy · Protein Interaction · Proteomics

Introduction

Protein–protein interaction is of fundamental importance for living organisms and provides unique possibilities to fine tune biological systems at molecular level. Delineating the fine details of interaction sites has thus been the motivation of significant research activities in the past (Lakey and Raggett 1998). NMR spectroscopy has contributed significantly in this area and despite considerable methodological progress there is, however, still a demand for improvement of the NMR experimental techniques with respect to sensitivity, automation capabilities, and protein consumption (Zuiderweg 2002).

In this article, we introduce a rapid and sensitive NMR-based approach for mapping protein–protein interaction sites using competition experiments based on our recently published NMR protein–protein interaction assay (Fig. 1) (Ludwiczek et al. 2004). In this assay the protein binding partner of interest is linked to a ligand binding domain (e.g. a SH2-domain) with moderate or medium affinity to a well-defined small molecule ligand (e.g. phenylphosphate), which serves as a model compound for the natural ligand phosphotyrosine. Protein–protein interaction is indirectly observed via subsequent NMR relaxation changes (e.g. selective T_1or T_2) of the reversibly binding ligand, caused by the increase in the molecular weight of the complex. Note that this method will not work using non-selective T_1

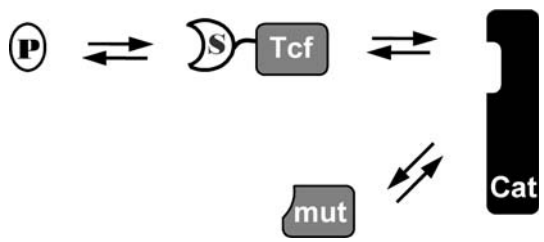

Fig. 1 Outline of the NMR-based mapping of Tcf4/β-Catenin interaction sites using competition binding experiments. Phenylphosphate (P) is used as a reporter ligand which reversibly binds to the ligand-binding domain SH2 (S) that is fused to the wild type target protein (Tcf). Changes in the molecular weight of the complex that occur either upon binding of tagged wild type SH2-Tcf4 to β-Catenin (Cat) or upon replacement of the tagged wild-type from the complex by an untagged mutant (mut) with certain binding affinity are both monitored via changes in relaxation rates of the ligand P

B. Baminger · G. Kontaxis · R. Konrat (✉)
Department of Biomolecular Structural Chemistry, Max F. Perutz Laboratories, University of Vienna, Vienna 1030, Austria
e-mail: robert.konrat@univie.ac.at

M. L. Ludwiczek
Department of Biochemistry and Molecular Biology, University of British Columbia, Vancouver, BC, CanadaV6T 1Z3

S. Knapp
Structural Genomics Consortium (SGC), Botnar Research Centre, University of Oxford, Oxford OX3 7LD, UK

(or T_2) measurements as only selective relaxation rates are proportional to $J(0)$ and τ_c. This indirect observation strategy avoids any molecular weight limit as in the case of direct NMR observation of the protein and significantly reduces the amount of protein material required, a general bottleneck for biological applications of NMR spectroscopy.

Here we demonstrate a first systematic competition binding application of this NMR methodology for mapping the protein–protein interaction site of the β-Catenin/Tcf4 protein complex, an important constituent of the Wnt signalling pathway and emerging drug development target. β-Catenin is an intracellular mediator in the Wnt signalling pathway and is thus interacting with proteins of the Tcf (T-cell factor)/Lef (lymphocyte enhancer binding factor) family of DNA binding proteins. In the absence of Wnt signalling, target genes are kept in a quiescent state by Tcf proteins (Cavallo et al. 1998; Roose et al. 1998), whereas under active signalling, cytosolic β-Catenin is transferred into the nucleus and together with Tcf proteins acts as transcriptional activator (Huber et al. 1996; Molenaar et al. 1996; Behrens et al. 1996; Nusse 1997; Seidensticker and Behrens 2000; van de Wetering et al. 1997). Previous studies have revealed that the Catenin-binding-domain (CBD) of Tcf4, the human homologue of this protein family, is located in the 53 N-terminal amino acids, and this construct is both, necessary and sufficient for high affinity interaction with β-Catenin (Molenaar et al. 1996; Behrens et al. 1996; van de Wetering et al. 1997; Knapp et al. 2001). β-Catenin itself consists of a core region flanked by an N-terminal segment, which is required for degradation (Peifer and Polakis 2000), and a C-terminal segment that recruits transcriptional coactivators (Barker et al. 2000). The core region, which was used for this study, is composed of 12 copies of a 42 amino acid sequence motif called armadillo repeat and forms a superhelix of helices that features a long, positively charged groove and mediates the interaction with Tcf4 (Huber et al. 1997).

Materials and methods

The core region of β-Catenin comprising residues 134–671 was expressed using the *pGex-6p2* vector and *E. coli* strain BL21(DE3)pLysS. The GST fusion protein was purified using Glutathione Sepharose affinity and subsequent size exclusion chromatography. The GST tag was removed using Precision protease. Mutant forms of Tcf4 and the fusion protein SH2-Tcf4 were prepared as described elsewhere (Ludwiczek et al. 2004; Fasolini et al. 2003). Selective inversion and excitation in the NMR relaxation experiments were achieved using IBURP (pulse width: 54 ms) and EBURP (pulse width: 50 ms) pulse shapes, respectively (Geen and Freeman 1991). Sample concentrations were as follows: phenylphosphate: 400 μM; β-Catenin: 75 μM; SH2-Tcf4: 75 μM; wt-Tcf4: 75μM and 750 μM. Experiments were performed on a Varian Unity Inova 500 MHz spectrometer. Spectra were acquired with 16 transients each using a relaxation delay of 5 s between scans. Sample conditions: pH 7.4, 1 mM DTT, T = 25°C. The NMR interaction data were independently cross-validated using size exclusion chromatography. For these experiments equimolar amounts of β-Catenin, SH2-Tcf4, and the respective competing Tcf4 mutant were loaded onto a HiLoad 16/60 Superdex Column. As a running buffer PBS buffer, pH 7.4 was used for the size exclusion experiments.

Results and discussion

Binding of the reporter ligand phenylphosphate to the SH2 domain in the SH2-Tcf4 fusion protein and/or the SH2-Tcf4/β-Catenin complex was monitored by selective T_1 relaxation ($T_{1,s}$) measurements. Figure 2 shows the results of $T_{1,s}$ experiments obtained for the intact SH2-Tcf4/β-Catenin complex and the competition binding experiments using wild-type (wt) Tcf4 protein, respectively. Competition binding experiments were performed with equimolar amounts and a 1:10 excess of wt-Tcf4, which replaced SH2-tagged Tcf4 in the SH2-Tcf4/β-Catenin complex thus

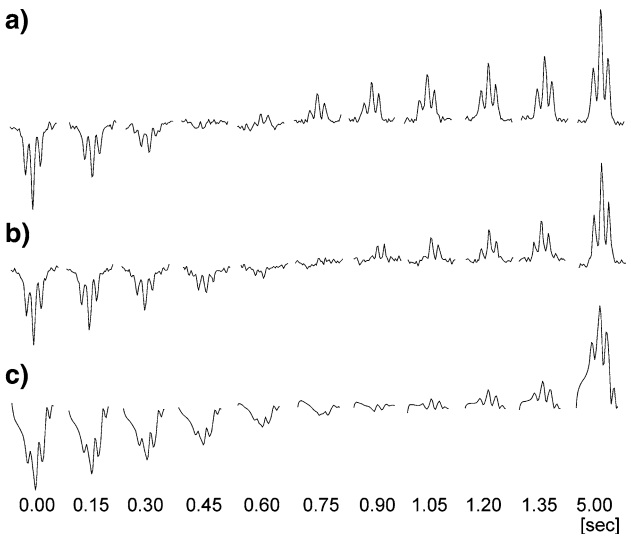

Fig. 2 Experimental demonstration of ligand-detected NMR protein–protein competition binding. The binding of wt-Tcf4 protein to β-Catenin is indirectly monitored by changes in the $T_{1,s}$ values. $T_{1,s}$-recovery curves of the meta proton of phenylphosphate reversibly bound to SH2-Tcf4/β-Catenin in (**a**) absence of , (**b**) presence of 1:1 ratio wt-Tcf4 and (**c**) 1:10 ratio of wt-Tcf4

reducing the average molecular weight of the (ligand binding) SH2-Tcf4 fusion protein and increasing the $T_{1,s}$ values.

To map Tcf4/β-Catenin protein–protein interaction sites Ala positional scanning was monitored by NMR competition binding experiments. The following Tcf4 mutants were investigated: D10A, D16A, I19A, F21A, E24A, and V44A. The competition efficiency of a particular mutant was measured by comparing the resulting selective R_1 rates ($R_{1,s} = 1/T_{1,s}$) with the values obtained for wt-Tcf4. First, the replacement of SH2-Tcf4 in the complex by wt-Tcf4 was tested (Fig. 3a). Increasing concentrations of wt-Tcf4 lead to continous substitution of SH2-Tcf4 by wt-Tcf4 in the Tcf4/β-Catenin complex and thus a reduction of $R_{1,s}$. Accordingly, the selective relaxation rate of the reporter ligand proton is shifted from the bound state of SH2-Tcf4 (meaning bound to β-Catenin) towards the unbound (free) state of SH2-Tcf4. Virtually complete replacement of SH2-Tcf4 was observed with a 10-fold access of untagged Tcf4 (relative to SH2-Tcf4). At this concentration the observed $R_{1,s}$ rate corresponds to that of the free form of SH2-Tcf4.

Next, competition binding experiments were performed with SH2-Tcf4/β-Catenin and equimolar amounts of Tcf4 mutants (Fig. 3b). Out of the six mutants studied, D16A and F21A showed the largest loss in competition binding, followed by V44A, D10A and I19A. E24A exhibited the smallest change in $R_{1,s}$ rate, indicating that the mutation of Glutamate to Alanine at this position of Tcf4 does not significantly influence the affinity between Tcf4 and β-Catenin. These findings are in very good agreement with independent isothermal calorimetry (ITC) studies (Fasolini et al. 2003). Their ITC analysis revealed the largest reduction in binding constant for mutant D16A. Based on the crystal structure of Tcf4/β-Catenin and on mutagenesis data on β-Catenin this was explained by an intricate interaction network formed between β-Catenin residues K435, N426, H470, R469, and K508 and the Tcf4 residues D16 to I19 (von Kries et al. 2000). The impaired β-Catenin binding of mutants D10A and V44A could also be explained by the crystal structure of the complex (Graham et al. 2001). Tcf4 residue D10 forms a salt bridge with β-Catenin residue R612, while V44 is located in an amphipathic helix and thus being involved in hydrophobic intermolecular contacts. Finally, residue E24 is pointing towards the solvent and thus not part of the binding interface. Consistently, no significant change in competition binding was found in the NMR experiments for mutant E24A. The only observed contradiction to previous ITC measurements was a significant loss in binding competence of mutant F21A.

The NMR findings were subsequently independently cross-validated and corroborated by applying size exclusion chromatography to separate solutions of Tcf4/β-Catenin complexes containing either tagged (SH2) or untagged Tcf4 proteins, respectively (Fig. 4). While wt-Tcf4 and Tcf4 mutant E24A replace SH2-Tcf4 in the β-Catenin complex and thus a separate peak of SH2-Tcf4 can be observed in the chromatogram, Tcf4 mutant F21A looses its binding affinity for β-Catenin and is not able to significantly replace SH2-Tcf4 in the complex. Further

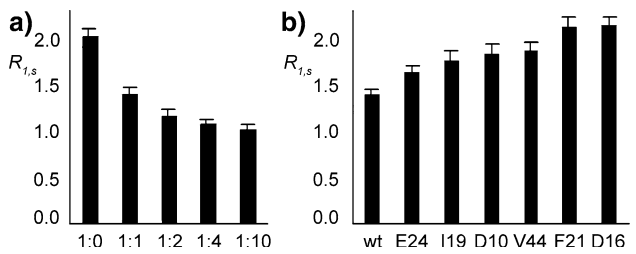

Fig. 3 Experimental $R_{1,s}$ rates obtained in competition binding experiments. (**a**) Selective relaxation rates of phenylphosphate bound to SH2-Tcf4/β-Catenin in absence of (1:0) and presence of 1:1, 1:2, 1:4, 1:10 ratios of wt-Tcf4. The $R_{1,s}$ rate at 10-fold molar access approaches the rate of the free form, indicating nearly complete substitution of SH2-Tcf4 in the complex. (**b**) NMR-detected Ala mutational scanning of the β-Catenin binding site in Tcf4. Relaxation rates of phenylphosphate bound to SH2-Tcf4/β-Catenin in the presence of a 1:1 molar ratio of wt-Tcf4 (wt) and Tcf4 mutants E24, I19, D10, V44, F21, and D16, respectively. The decrease in $R_{1,s}$ is used as an indicator for the relative binding efficiency of the individual Tcf4 mutants (see text). Errors were estimated based on a Monte Carlo analysis

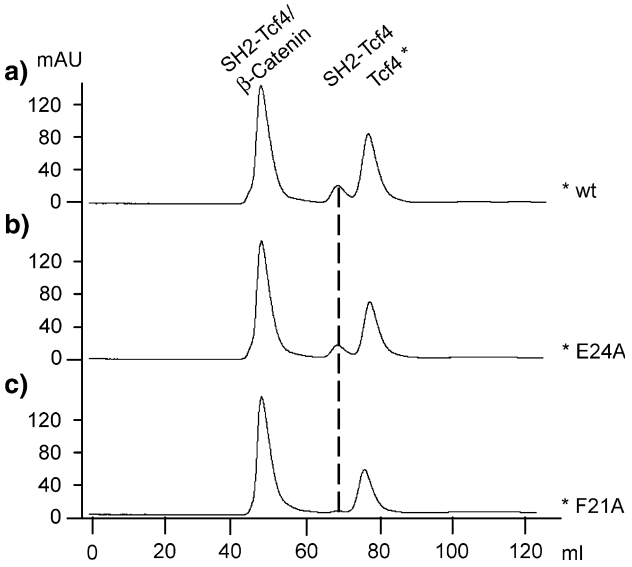

Fig. 4 Cross-validation of NMR findings using size exclusion chromatography. Mixtures of SH2-Tcf4/β-Catenin and equimolar amounts of (**a**) wt-Tcf4, (**b**) Tcf4 mutant E24A, and (**c**) Tcf4 mutant F21A were loaded onto a HiLoad 16/60 Superdex Column. As seen from (**a**) and (**b**) wt-Tcf4 and mutant E24A displace SH2-Tcf4 from the β-Catenin complex and the mixture separates into three peaks, while (**c**) Tcf4 mutant F21A does not displace SH2-Tcf4 from the SH2-Tcf4/β-Catenin complex.

evidence for the importance of residue F21 comes from yeast-two hybrid experiments obtained with the related transcription factor Lef1 and transfection experiments in which a 40% loss of function was observed for the double mutant I19A, F21A (Fasolini et al. 2003). In the crystal structure of the β-Catenin/Tcf4 complex (Graham et al. 2001), F21 is deeply buried in the complex interface, not solvent-accessible, and involved in hydrophobic interactions between β-Catenin and Tcf4 (Fig. 5). The changes in the binding affinity of mutant F21A found by our NMR measurements are therefore not unexpected and supported by structural data.

Conclusion

In conclusion, we have shown that protein–protein interaction sites can be efficiently mapped using indirect NMR reporter monitoring. The particular benefit of this methodology is significantly reduced protein consumption compared to other methods such as ITC. Furthermore, the methodology does not require sophisticated isotope labelling of proteins or complicated multi-pulse NMR experiments. It is very fast (experimental time for a single $T_{1,s}$ recovery measurement is on the order of about 15 min), straightforward to implement and easy to interpret. In the future, further improvements concerning sensitivity could be envisaged by applying homonuclear band-selective decoupling during acquisition. It should be noted that the SH2-domain, which is used as the ligand binding domain in those NMR experiments, significantly facilitates the purification of the fusion protein. It can easily be used as a purification tag for ion exchange chromatography during the purification procedure. The proteins for the competition experiments, however, remain untagged and can be purified as usual. Concerning the length of the flexible linker between the SH2 domain and the target protein, care has to be taken as too long linkers can promote independent tumbling of the two protein domains and renders monitoring of molecular weight induced relaxation changes unfeasible. However, the NMR relaxation analysis of the multi-domain protein CRP2 revealed significant correlation time changes despite the largely independent reorientational motional dynamics of the two individual LIM domains (Konrat et al. 1998). Specifically, the correlation times of the two LIM domains (separated by a flexible 58-amino acid linker region) were significantly larger in full-length CRP2 (7.4 ns) compared to the isolated amino-terminal LIM1 (5.6 ns) and carboxy-terminal LIM2 domain (6.2 ns), respectively. We thus conclude that the linker length does not critically impair the performance of the experiment.

Extensions to large biological systems are feasible and straightforward. For example, preliminary experiments in our laboratory have demonstrated applications of the methodology to molecular systems as large as intact viruses (unpublished results). We thus anticipate widespread applications of the method for automated protein–protein interaction site mapping.

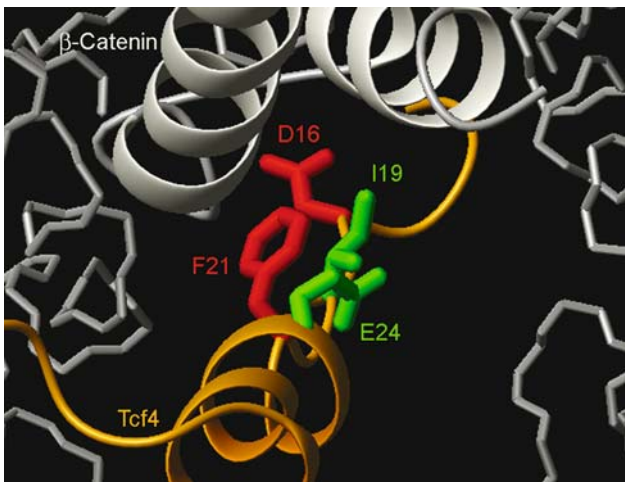

Fig. 5 Mapping of the protein–protein binding site in the Tcf4/β-Catenin complex. Annotation as interaction relevant residue was based on experimental $R_{1,s}$ changes in competition binding experiments. Tcf4 mutants D16A and F21A alter residues pointing towards the Tcf4/β-Catenin interface (red). They result in large changes in the NMR detected $R_{1,s}$ rates, which is indicative for a significant loss in competition efficiency. In contrast, in Tcf4 mutants I19A and E24A the altered residues (green) do not directly interact with β-Catenin and show only moderate changes in the $R_{1,s}$ relaxation rates. The figure was prepared from the β-Catenin/Tcf4 crystal structure, pdb: 1JDH (Graham et al. 2001) using Molmol (Koradi et al. 1996).

Acknowledgements We thank Prof. Julie Forman-Kay (University of Toronto) for the plasmid encoding for the SH2 domain of PLCγ1. This work is supported by grant WWTF, LS162.

References

Barker N, Morin PJ, Clevers H (2000) The Yin-Yang of TCF/beta-catenin signaling. Adv Cancer Res 77:1–24

Behrens J, von Kries JP, Kuhl M, Bruhn L, Wedlich D, Grosschedl R, Birchmeier W (1996) Functional interaction of beta-catenin with the transcription factor LEF-1. Nature 382:638–642

Cavallo RA, Cox RT, Moline MM, Roose J, Polevoy GA, Clevers H, Peifer M, Bejsovec A (1998) Drosophila Tcf and Groucho interact to repress Wingless signalling activity. Nature 395: 604–608

Fasolini M, Wu X, Flocco M, Trosset JY, Oppermann U, Knapp S (2003) Hot spots in Tcf4 for the interaction with beta-catenin. J Biol Chem 278:21092–21098

Geen H, Freeman R (1991) Band-selective radiofrequency pulses. J Magn Res 93:93–141

Graham TA, Ferkey DM, Mao F, Kimelman D, Xu W (2001) Tcf4 can specifically recognize beta-catenin using alternative conformations. Nat Struct Biol 8:1048–1052

Huber AH, Nelson WJ, Weis WI (1997) Three-dimensional structure of the armadillo repeat region of beta-catenin. Cell 90:871–882

Huber O, Korn R, McLaughlin J, Ohsugi M, Herrmann BG, Kemler R (1996) Nuclear localization of beta-catenin by interaction with transcription factor LEF-1. Mech Dev 59:3–10

Knapp S, Zamai M, Volpi D, Nardese V, Avanzi N, Breton J, Plyte S, Flocco M, Marconi M, Isacchi A, Caiolfa VR (2001) Thermodynamics of the high-affinity interaction of TCF4 with beta-catenin. J Mol Biol 306:1179–1189

Konrat R, Kräutler B, Weiskirchen R, Bister K (1998) Structure of cysteine-and glycine-rich protein CRP2. Backbone dynamics reveal motional freedom and independent spatial orientation of the lim domains. J Biol Chem 273(36):23233–23240

Koradi R, Billeter M, Wuthrich K (1996) MOLMOL: a program for display and analysis of macromolecular structures. J Mol Graph 14:51-5, 29–32

Lakey JH, Raggett EM (1998) Measuring protein-protein interactions. Curr Opin Struct Biol 8:119–123

Ludwiczek ML, Baminger B, Konrat R (2004) NMR probing of protein-protein interactions using reporter ligands and affinity tags. J Am Chem Soc 126:1636–1637

Molenaar M, van de Wetering M, Oosterwegel M, Peterson-Maduro J, Godsave S, Korinek V, Roose J, Destree O, Clevers H (1996) XTcf-3 transcription factor mediates beta-catenin-induced axis formation in Xenopus embryos. Cell 86:391–399

Nusse R (1997) A versatile transcriptional effector of Wingless signaling. Cell 89:321–323

Peifer M, Polakis P (2000) Wnt signaling in oncogenesis and embryogenesis-a look outside the nucleus. Science 287:1606–1609

Roose J, Molenaar M, Peterson J, Hurenkamp J, Brantjes H, Moerer P, van de Wetering M, Destree O, Clevers H (1998) The Xenopus Wnt effector XTcf-3 interacts with Groucho-related transcriptional repressors. Nature 395:608–612

Seidensticker MJ, Behrens J (2000) Biochemical interactions in the wnt pathway. Biochim Biophys Acta 1495:168–182

van de Wetering M, Cavallo R, Dooijes D, van Beest M, van Es J, Loureiro J, Ypma A, Hursh D, Jones T, Bejsovec A, Peifer M, Mortin M, Clevers H (1997) Armadillo coactivates transcription driven by the product of the Drosophila segment polarity gene dTCF. Cell 88:789–799

von Kries JP, Winbeck G, Asbrand C, Schwarz-Romond T, Sochnikova N, Dell'Oro A, Behrens J, Birchmeier W (2000) Hot spots in beta-catenin for interactions with LEF-1, conductin and APC. Nat Struct Biol 7:800–807

Zuiderweg ER (2002) Mapping protein-protein interactions in solution by NMR spectroscopy. Biochemistry (Mosc) 41:1–7